This article was downloaded by: [Institute Of Atmospheric Physics]
On: 09 December 2014, At: 15:30
Publisher: Taylor & Francis
Informa Ltd Registered in England and Wales Registered Number: 1072954 Registered office: Mortimer House, 37-41 Mortimer Street, London W1T 3JH, UK

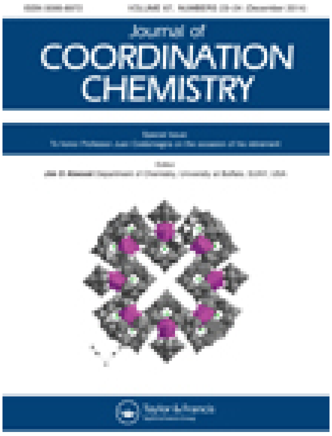

Journal of Coordination Chemistry
Publication details, including instructions for authors and subscription information:
http://www.tandfonline.com/loi/gcoo20

In search for chelating TAMLs (tetraamido macrocyclic ligands) with peripheral bidentate donor centers: a cobalt(III) complex of the 3,3′-(2,2′-bipyridindiyl)-tailed TAML

Rafael Omar Saavedra Díaz[a], Ronan Le Lagadec[a], Longzhu Q. Shen[b] & Alexander D. Ryabov[b]

[a] Instituto de Química, UNAM, México D.F., Mexico

[b] Department of Chemistry, Carnegie Mellon University, Pittsburgh, PA, USA

Accepted author version posted online: 10 Sep 2014.Published online: 03 Oct 2014.

Click for updates

To cite this article: Rafael Omar Saavedra Díaz, Ronan Le Lagadec, Longzhu Q. Shen & Alexander D. Ryabov (2014) In search for chelating TAMLs (tetraamido macrocyclic ligands) with peripheral bidentate donor centers: a cobalt(III) complex of the 3,3′-(2,2′-bipyridindiyl)-tailed TAML, Journal of Coordination Chemistry, 67:23-24, 3909-3919, DOI: 10.1080/00958972.2014.964224

To link to this article: http://dx.doi.org/10.1080/00958972.2014.964224

PLEASE SCROLL DOWN FOR ARTICLE

Taylor & Francis makes every effort to ensure the accuracy of all the information (the “Content”) contained in the publications on our platform. However, Taylor & Francis, our agents, and our licensors make no representations or warranties whatsoever as to the accuracy, completeness, or suitability for any purpose of the Content. Any opinions and views expressed in this publication are the opinions and views of the authors, and are not the views of or endorsed by Taylor & Francis. The accuracy of the Content should not be relied upon and should be independently verified with primary sources of information. Taylor and Francis shall not be liable for any losses, actions, claims, proceedings, demands, costs, expenses, damages, and other liabilities whatsoever or howsoever caused arising directly or indirectly in connection with, in relation to or arising out of the use of the Content.

This article may be used for research, teaching, and private study purposes. Any substantial or systematic reproduction, redistribution, reselling, loan, sub-licensing,

Journal of Coordination Chemistry, 2014
Vol. 67, Nos. 23–24, 3909–3919, http://dx.doi.org/10.1080/00958972.2014.964224

In search for chelating TAMLs (*t*etra*a*mido *m*acrocyclic *l*igands) with peripheral bidentate donor centers: a cobalt(III) complex of the 3,3′-(2,2′-bipyridindiyl)-tailed TAML

RAFAEL OMAR SAAVEDRA DÍAZ†, RONAN LE LAGADEC*†,
LONGZHU Q. SHEN‡ and ALEXANDER D. RYABOV‡

†Instituto de Química, UNAM, México D.F., Mexico
‡Department of Chemistry, Carnegie Mellon University, Pittsburgh, PA, USA

(*Received 10 June 2014; accepted 26 August 2014*)

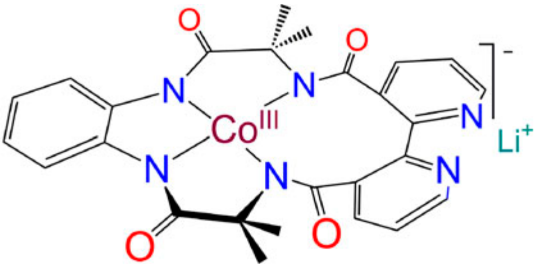

The synthesis of 1,2-$C_6H_4(NHCOCMe_2NHCO)_2$-3,3′-(2,2′-bpy) (**3**), a TAML (*t*etra*a*mido *m*acrocyclic *l*igand) incorporating the peripheral 2,2′-bipyridine unit, is described. Its geometry after optimization by density functional theory (DFT) indicated a rather unfavorable conformation of four N–H amide units for forming macrocyclic transition metal complexes. This explains why the iron(III) derivative of **3** could not be obtained even after deprotonation of the N–H bonds by *n*-BuLi. Nevertheless, the macrocyclic complex of Co^{III} was synthesized in moderate yield, characterized, and explored by DFT. Our data suggest a strongly distorted square-planar geometry of the macrocyclic complex between Co^{III} and **3**. The dihedral angle between the pyridine rings equals 80° ruling out the possibility of metal chelation by the bipyridine unit.

Keywords: Macrocyclic complex; TAML; DFT calculations; Cobalt complex

1. Introduction

The chemistry of metal complexes of TAMLs (*t*etra*a*mido *m*acrocyclic *l*igands) is a rapidly developing area of modern applied and academic research [1–5]. Attention to these compounds and particularly to the iron derivatives is inspired by their exceptional reactivity

---

*Corresponding author. Email: ronan@unam.mx.

Dedicated to Prof. Juan Costamagna, a long-time Editorial Board member who is retiring in December 2014.

in peroxidase-like oxidations by hydrogen peroxide, together with their prominent operational stability and resistance to self-destruction during the catalysis [6, 7]. In particular, iron TAMLs catalyze the oxidative bleaching of various dyes, destruction of polychlorinated phenols and nitroaromatics, purification of drinking water by, *inter alia*, efficient decontamination of drugs, and endocrine disruptors. The catalysts convert different molecules into small non-toxic fragments, which is their greatest advantage. Deep fragmentation was shown for polychlorophenols, the fenitrothion pesticide, Orange II, and pinacyanol chloride dyes [3–5]. Fields of application are truly vast and this inspires research to synthesize TAMLs with new structural elements [8–10] for solving specific academic and technological goals.

Using immobilized TAML catalysts on solid supports is an attractive technological application. However, unlike cobalt(II) porphyrin or phthalocyanine macrocycles, which have extensively been studied by Costamagna and co-workers and were shown to be easily attachable to electrode surfaces [11–13], studies on the immobilization of TAML derivatives are limited [14, 15]. There are numerous routines for the preparation of heterogeneous catalysts, including coordinative immobilization [16]. To achieve this, TAMLs should contain peripheral coordinative centers (sites). Additional advantage of this approach is that it allows coordination of other metal units to the peripheral sites and by such to tune electronic and steric features of the catalysts. The first step in this direction was made in the late 1990s when the "head" aryl group of the prototype TAML **1** was replaced by the pyridine functionality (figure 1) [17]. TAML **2** is potentially a peripheral bidentate ligand due to the pyridine nitrogen and the adjacent amide oxygen. Needless to say the oxygen is a poor donor center and therefore alternative options for introducing stronger donor centers should be explored. For this reason, it was decided to design TAML containing a peripheral 2,2′-bipyridine unit such as **3** which could be advantageous when compared to **2**.

In this work, a complexation between cobalt(III) and ligand **3** was investigated. "Trivalent Co is one of the most thoroughly investigated ions in transition metal chemistry … Six-coordinate octahedral geometry is particularly dominant in this oxidation state … Despite a century of exploration cobalt(III) chemistry continues to reward and surprise the investigator." These words have opened the chapter "Cobalt" by Bernhardt and Lawrence in Volume 6 of *Comprehensive Coordination Chemistry II* [18]. Square-planar configurations of Co^{III} are significantly less common than octahedral [18] and therefore the synthesis of **4** is a valid contribution to this field. Square-planar 14-electron Co^{III} complexes are electron deficient species. Their axial sites are opened for various molecules and therefore the complexes are involved in different catalytic processes such as asymmetric epoxidations by iodosylbenzene [19] and air [20] or hydrogenation of alkenes [21]. They are viewed as mimics of the metal core of the cobalt containing nitrile hydratase enzymes [22–25]. In fact,

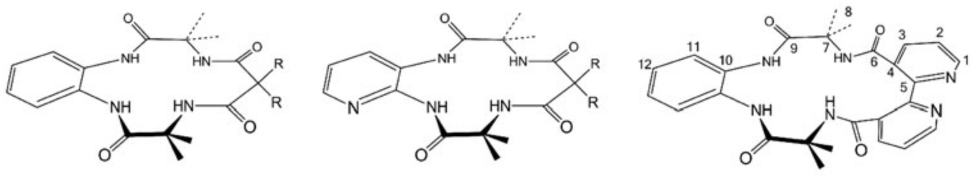

1 2 3

Figure 1. Structure of previously prepared TAMLs and of new ligand **3**.

nitrile hydratase from *Pseudonocardia thermophila* JCM 3095 contains Co^{III} stabilized by two amide nitrogens [26]. Moreover, Co^{III} complex of **1** was recently shown to catalyze cycloaddition of CO_2 to epoxides [27]. Therefore in this contribution we describe the synthesis of TAML **3**, its complexation with cobalt(III), characterization of the products formed, and investigation of the new molecules by density functional theory (DFT) methods.

2. Experimental

2.1. *Materials and methods*

The ^{1}H (300.53 MHz) and $^{13}C\{^{1}H\}$ (75.56 MHz) NMR spectra were recorded on a JEOL GX300 spectrometer in DMSO-d_6 or CD_3OD. Chemical shifts (δ) and coupling constants (J) are expressed in ppm and Hz, respectively. Two-dimensional shift-correlated experiments (COSY, HETCOR) were used to unambiguously assign the chemical shifts. Elemental analyses were carried out in an Elementar Vario Micro Cube. EPR measurements were made with a Jeol JES-TE300 spectrometer. IR spectra were recorded on a Bruker-Alpha ATR apparatus. UV–vis spectra in methanol were obtained using a Shimadzu 2700 spectrophotometer. Electrospray ionization mass spectra (ESI-MS) were obtained using a Bruker Esquire spectrometer. Electrochemical measurements were performed on a PC-interfaced potentiostat–galvanostat AUTOLAB PGSTAT 12.

All chemicals were purchased from Sigma–Aldrich and used without purification. All preparative procedures were carried out under dry nitrogen or argon using standard Schlenk techniques. The solvents were distilled from appropriate drying agents under nitrogen. 2-Methyl-2-phthalimidopropanoyl chloride **A** [28], *N*,*N*′-(1,2-phenylene)bis(2-(1,3-dioxoisoindolin-2-yl)-2-methylpropanamide **B** [29], *N*,*N*′-(1,2-phenylene)bis(-amino-2-methylpropanamide) **C** [29], and 3,3′-dicarboxybipyridine acid [30, 31] were prepared as previously described. The $[Co(CH_3CN)_6](BF_4)_2$ precursor was synthesized according to the literature procedure [32].

2.2. *Synthesis of [2,2′-Bipyridine]-3,3′-dicarbonyl dichloride hydrochloride (D)*

A solution of 1.0 g (4.1 mM) of 3,3′-dicarboxybipyridine acid in 4 mL of thionyl chloride was stirred under argon at room temperature for 12 h. Thionyl chloride was removed under reduced pressure and 5 mL of diethyl ether was added to the flask. The precipitate was filtered off and washed three times with diethyl ether to eliminate residues of $SOCl_2$. The white solid was dried under vacuum. Yield: 94% (1.36 g). ^{1}H NMR (DMSO-d_6) 8.85 (dd, 2 H, $^{2}J = 5.0$, $^{3}J = 1.5$, **H1**), 8.54 (dd, 2 H, $^{2}J = 7.9$, $^{3}J = 1.5$, **H3**), 7.78 (dd, 2 H, $^{2}J = 7.9$, $^{2}J = 5.0$, **H2**). FT-IR (cm^{-1}) 2454 (NH), 1711 (CO).

2.3. *Synthesis of TAML 3*

A mixture of 1.0 g (3.6 mM) of **C**, 1.27 g (3.6 mM) of **D**, and 2.0 mL (14.4 mM) of Et_3N in 20 mL of dry THF was stirred at 50 °C for 72 h. The mixture was cooled to room temperature and the solvent was removed under reduced pressure. The white residue was suspended in 10 mL acetone and filtered off. The product was first washed with 10 mL of 2-propanol, then the remaining solid was stirred in 5 mL of 9 : 2 acetone : water mixture to assure complete elimination of $[Et_3NH]Cl$. The white powder was finally washed several times with diethyl ether and dried at 80 °C for 5 h under vacuum. Yield: 65% (1.13 g). ^1H NMR (CD_3OD) 8.55 (d, 2 H, $^2J = 4.8$, **H1**), 8.21 (d, 2 H, $^2J = 7.8$, **H3**), 7.52 (dd, 2 H, $^2J = 6.1$, $^2J = 3.5$, **H11**), 7.45 (dd, 2 H, $^2J = 7.8$, $^2J = 4.9$, **H2**), 7.30 (dd, 2 H, $^2J = 6.1$, $^2J = 3.5$, **H12**), 1.64 (s,12 H, **H8**). ^{13}C NMR (CD_3OD) 172.01 (CO, **C9**), 171.18 (CO, **C6**), 157.60 (**C5**), 148.45 (**C1**), 137.54 (**C3**), 132.38 (**C10**), 130.42 (**C4**), 126.33 (**C12**), 125.76 (**C11**), 122.70 (**C2**), 56.77(**C7**), 23.81 (**C8**). IR (cm^{-1}): 3253 (NH), 1659 (CO), 1593 (CO). UV–vis (MeOH): $\lambda_{max} = 242$ nm, $\varepsilon = 13{,}500\ M^{-1}\ cm^{-1}$. ESI-MS (positive mode): *m/z* 558 $[M + THF]^+$. Anal. Calcd for $C_{26}H_{26}N_6O_4 \cdot 2.5H_2O$ (%): C, 58.75; H, 5.88; N, 15.81. Found (%): C, 59.03; H, 5.53; N, 15.71.

2.4. *Preparation of 4*

Ligand **3** (50 mg, 0.1 mM) was dissolved in 10 mL of dry THF at 0 °C and 0.25 mL (0.4 mM) of *n*-BuLi (1.6 M in hexane) was added dropwise. The solution was stirred for 20 min and allowed to reach room temperature. The reaction mixture was cooled to 0 °C, $[Co(CH_3CN)_6](BF_4)_2$ (48 mg, 0.1 mM) added, and the mixture was stirred for 18 h at room temperature. A green brownish precipitate was formed. Air was bubbled through the solution for 2 h and the precipitate turned brown. The suspension was filtered through Celite. The precipitate was first washed with THF and acetonitrile before elution with ethanol. The solvent was evaporated and the green-brownish solid was washed with 3 mL of 9 : 1 acetone : water mixture to eliminate remaining lithium salts, washed with diethyl ether, and dried under reduced pressure. Yield: 40% (23 mg). ^1H NMR (CD_3OD) 8.76 (dd, 2 H, $^2J = 5.8$, $^2J = 3.0$, **H11**), 8.47 (d, 2 H, $^2J = 3.6$, **H1**), 8.15 (br d, 2 H, $^2J = 7.5$, **H3**), 7.44 (br, 2 H, **H2**), 6.95 (dd, 2 H, $^2J = 5.8$, $^2J = 3.0$, **H12**), 1.53 (s,12 H, **H8**). ^{13}C NMR (CD_3OD) 179.98 (CO, **C9**), 173.38 (CO, **C6**), 157.65 (**C5**), 147.21(**C1**), 144.17 (**C10**), 136.65(**C3**), 135.47 (**C4**), 122.45 (**C2**), 122.13 (**C12**), 120.90 (**C11**), 56.91(**C7**), 27.95 (**C8**). IR (cm^{-1}): 1595 (CO), 1575 (CO). UV–vis (MeOH), $\lambda_{max} = 260$ and 295 nm, $\varepsilon = 12{,}800$ and 6100 $M^{-1}\ cm^{-1}$, respectively. ESI-MS (negative mode): *m/z* 541 $[M]^-$. Anal. Calcd for $C_{26}CoH_{22}LiN_6O_4 \cdot 4.5H_2O$ (%): C, 49.61; H, 4.96; N, 13.35. Found (%): C, 49.78; H, 4.91; N, 13.05.

2.5. *Computational details*

The DFT calculations were performed with Gaussian 09 rev.B.01 [33] using Becke's three parameter hybrid functional [34, 35] along with the Lee–Yang–Parr correlation functional [36] and basis set 6-311G. This approach appeared to be very reliable for DFT studies of TAML complexes [37]. The geometries for **4** were obtained by full optimization in the gas phase until the default convergence criteria were met. The multiplicity of **4** was set to 1 in accordance with the ESR evidence. The initial model of **4** was built using the previously reported X-ray structural data for the Co^{III} complex of TAML **1** [27]. Multiple conformers were computed and the one with the lowest energy was reported. Calculations for ligand **3** were done both in the gas phase and THF solution by invoking the implicit continuum solvent model [38].

3. Results and discussion

3.1. *Synthesis and DFT analysis of TAML ligand 3*

TAML ligand **3** was prepared in five steps as shown in scheme 1. The synthesis was based on the methodology previously developed by Collins and co-workers [39], and **3** was characterized by ^{1}H and ^{13}C NMR, ESI-MS, IR, and UV–vis spectroscopies, and elemental analysis. Analytical data showed that despite prolonged drying under vacuum, water molecules remained attached to the compound. A peak corresponding to water at δ 1.74 is also present in the ^{1}H NMR spectrum. Characteristic carbonyl stretching frequencies can be observed at 1659 and 1593 cm^{-1} together with the N–H stretching at 3253 cm^{-1} in the IR spectrum of **3**. The ^{1}H NMR spectra of **3** obtained in DMSO-d$_6$ or methanol-d$_4$ contained a single peak at δ 1.64 from all four methyl groups of **3**. This strongly suggests fluxional behavior of the ligand in solution because the DFT-optimized structure of **3**, shown in figure 2 (*vide infra*), indicates clearly the non-equivalence of the methyl groups. There are just five groups of resonances from the aromatic hydrogens and this is also consistent with rapid transitions between possible conformers. No amide resonances were observed which is, however, not unusual for this type of compound in polar water-containing solvents. It is very likely that pyridine nitrogens of **3** favor the hydrogen exchange processes.

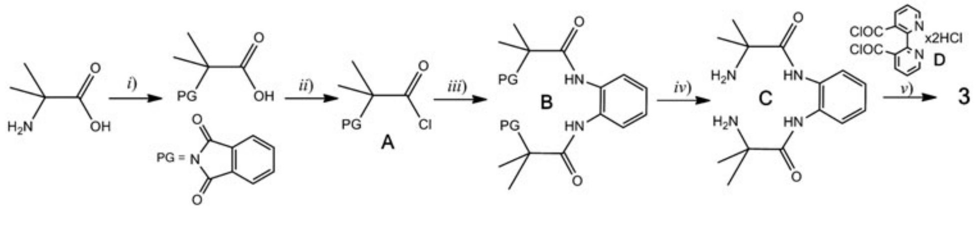

Scheme 1. Synthesis of **3**: *i*) NH_2 group protection, *ii*) acyl chloride formation, *iii*) double amidation, *iv*) deprotection, and *v*) ring-closure.

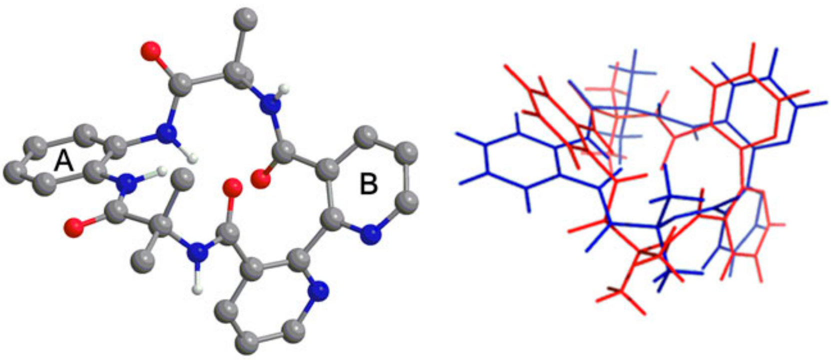

Figure 2. Left: DFT-optimized structure of **3** in the gas phase with only amide hydrogens shown for clarity (C in gray, N in blue, O in red, H in white). Right: overlay of the structures of **3** optimized in the gas phase (red) and in THF (blue) (see http://dx.doi.org/10.1080/00958972.2014.964224 for color version).

The optimization of the structure of **3** using DFT (figure 2) indicated that metalation of this TAML by a transition metal may not be easy. The ligand is highly distorted and just two of the four amide hydrogens are reasonably directed inside a potential ligand cavity. These are the hydrogens adjacent to the "head" aromatic ring of the ligand. The other two, which are closer to the "tail" part, are significantly diverted from the imaginary center of coordination. The dihedral angle of 80° between the two pyridine rings is also worth mentioning. This ligand feature might be a limiting factor for simple chelation of transition metals by the bipyridine unit of **3**.

The structures of **3** optimized in the gas phase and in THF solution are rather similar (figure 2, right). Both structures are strongly distorted. The amide hydrogens are directed divergently and the two pyridine rings of the bipyridine unit are almost orthogonal (70° and 80° for the gas phase and the THF solution, respectively). The gas phase structure is more globular. The angles between planes of rings A and B equal 95° and 102° in the gas phase and THF, respectively. Overall, the structural features of **3** in solid and solution are quite comparable.

3.2. *Synthesis and properties of cobalt(III) TAML complex 4, a derivative of 3*

TAML **3** does not react with $[Co(NCMe)_6](BF_4)_2$ in THF, suggesting that (*i*) the dihedral angle of 90° as in THF is an obstacle for the binding of Co^{II} to the bipyridine unit and (*ii*) Co^{II} is unable to metalate amide N–H bonds of **3**. The metalation was, however, realized in the presence of *n*-butyllithium as a strong base, which is known to lithiate TAMLs readily [1]. When the ligand was deprotonated by four equivalents of *n*-BuLi followed by addition of $[Co(NCMe)_6](BF_4)_2$, a highly unstable green solid precipitated, presumably a cobalt(II) complex, which after exposure to the air converted to a brown material, which was isolated in moderate yield (40%) and characterized by spectral and analytical data, which allowed assignment of the structure **4** (figure 3) to the newly prepared compound.

Different cobalt salts including $CoCl_2$, $CoCl_3$, and $Co(acac)_3$ were also used for the synthesis of **4**. In all cases, **4** was obtained in low yields (~20–30%) and the formation of salts as by-products complicated the purification. The cleanest reaction and the highest yield were achieved when $[Co(NCMe)_6](BF_4)_2$ was employed. The incorporation of cobalt has been confirmed by ESI-MS data. There are no N–H stretching bands in the IR spectrum of

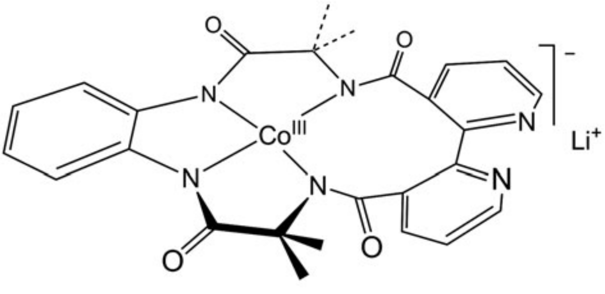

4

Figure 3. Proposed structure for cobalt(III) complex **4**.

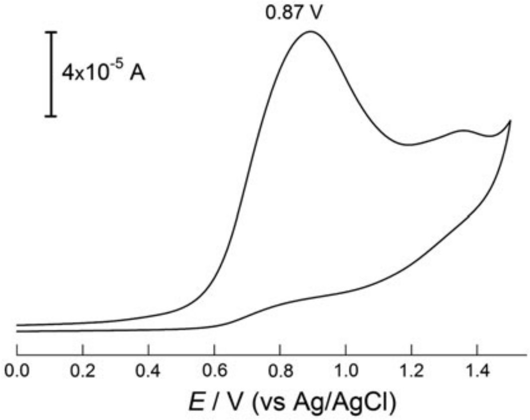

Figure 4. Cyclic voltammogram of **4** (1 mM) obtained in methanol in the presence of 0.1 M (n-Bu)$_4$NPF$_6$. Scan rate 100 mV s^{-1}, glassy carbon working electrode, and auxiliary Pt electrode.

4 and the carbonyl bands are now observed at 1595 and 1575 cm^{-1}, lower frequencies than in the free ligand **3**. The compound is EPR silent both at 77 K and room temperature, suggesting that **4** is a cobalt(III) derivative with $S = 0$. Diamagnetic features of **4** are consistent with ^{1}H and ^{13}C NMR data collected in methanol-d$_4$, though this was a challenge, because **4** is only slightly soluble in alcohols and is almost insoluble in other common organic solvents. This complicated the purification and made it impossible to grow crystals of **4** for X-ray investigation due to a strong tendency of **4** to precipitate from all solutions tested. Nevertheless, NMR spectra were obtained to reveal, similar to the ligand **3** case, just one set of signals. A plane of symmetry is very unlikely for **4** and therefore the complex should be extremely fluxional in solution at ambient conditions. There is one singlet resonance from all four methyl groups at δ 1.53 (*versus* at δ 1.64 for **3**). The resonances from aromatic hydrogens 11 and 12 (see figure 1 for the numbering scheme), which are the closest to cobalt(III), are also shifted to lower field for H11 ($\Delta\delta$ 1.24) and to higher field for H12 ($\Delta\delta$ 0.35), whereas the chemical shifts for the remaining aromatic protons remained practically unchanged. These observations are also consistent with the location of Co$^{\text{III}}$ inside the macrocycle.

Redox properties of **4** studied by cyclic voltammetry and presented in figure 4 did not prove to be promising. There is an irreversible oxidative feature seen around 0.87 V *versus* Ag/AgCl. This value lies in the range typical of Co$^{\text{III}}$ TAMLs and corresponds to the Co$^{\text{III}} \rightarrow$ Co$^{\text{IV}}$ transition [40, 41]. This process is reversible in TAML complexes which are much less distorted than **4** [40, 41].

Attempts to synthesize the corresponding iron(III) complex, analogous to various iron TAML derivatives possessing high catalytic activity in peroxidase-like reactions [3–5], were, however, unsuccessful. Using iron(II) precursors such as FeCl$_2$ and [Fe(NCMe)$_6$](BF$_4$)$_2$ the formation of a green precipitate was observed which then transformed into a red compound on exposure to air. The same red solid was obtained starting from iron (III) salts FeCl$_3$ and Fe(acac)$_3$. However, the red compound decomposed always upon purification as a result of demetalation. This is probably because iron(III) complexes are usually less robust than their cobalt counterparts and are more prone to hydrolysis and

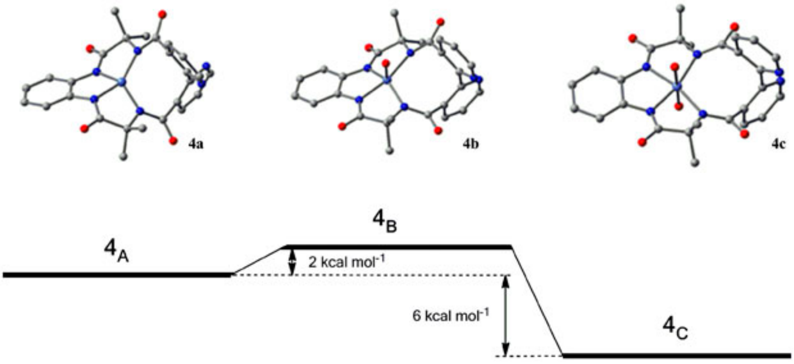

Figure 5. DFT-optimized structures of **4** assuming three coordinative modes of Co^{III}: square-planar (**4_A**), tetragonal pyramid (**4_B**), and octahedron (**4_C**). Donor centers of the "plane" are four deprotonated amide nitrogens; fifth and sixth sites are oxygens of aqueous ligands. Hydrogens are not shown for clarity. Below are the relative energies of **4_A**, **4_B**, and **4_C**.

reaction with oxygen [27]. It is also known that a distortion of the planar arrangement of deprotonated amide nitrogens around iron(III) make such TAML complexes very unstable to moisture [42].

3.3. *DFT optimizations of coordinative polyhedra of 4*

According to X-ray structural data of previously reported cobalt(III) TAML complexes, cobalt(III) surrounded by four deprotonated amide nitrogens of TAMLs adopts a square-planar geometry with distortion [27, 40, 41, 43]. Our spectroscopic data agree with such a structural model though it is natural to anticipate significantly larger distortions of the square plane in the case of TAML **3**. In the absence of crystallographic information, it was intriguing to predict theoretically the coordinative polyhedron of Co^{III} in **4**. Therefore, several DFT simulations of coordinative variants of **4** have been performed. Main results are shown in figure 5. Square plane of **4_A** is extremely distorted. The Co–N bond distances vary significantly from 1.85 to 1.91 Å, the longest bond being closer to the bipyridine unit. Amide nitrogens in octahedral (or square bipyramidal) model **4_C** built up by two axial aqueous ligands are significantly more planar than four-coordinate model **4_A** and the Co–N bond distances are 1.91–2.02 Å. Model **4_C** is more, by 6 kcal M^{-1}, energetically favored. Interestingly, the five-coordinate model **4_B** seems to be less advantageous energy-wise than **4_A**. The amide nitrogens of **4_B** are similarly distorted as in **4_A** and the Co–N bond distances are 1.85–2.02 Å, i.e. their variation is the largest for **4_B**. It is worth noting the Co–N bond distances are practically of the same length and equal to 1.82–1.83 Å in the undistorted Co^{III} complex with TAML **1** [27]. To this end, the stability of computed structures decreases in the series: **4_C** > **4_A** > **4_B**. The series gives some extra confidence with the assignment of cobalt(III) TAML as **4**. TAML complexes of Co^{III}, Ni^{III}, and Co^{IV} are four coordinate in the solid state in the absence of extra strongly coordinating ligands [27, 40, 41, 43]. TAML complexes of Fe^{III} and Fe^{IV} are five coordinate and never six as solids, provided the same condition holds. Thus, since **4_A** is more energetically advantageous than **4_B**, we assume that structural assignment of **4** as **4_A** seems to be the most probable.

Other observations worth mentioning are as follows. The dihedral angle between the pyridine rings is large in all three models, i.e. 97°, 85°, and 79° in $\mathbf{4_A}$, $\mathbf{4_B}$, and $\mathbf{4_C}$, respectively. Thus, it is rather problematic for the bipyridine unit of **4** to serve as a bidentate ligand. In addition to $\mathbf{4_A}$, we have found a configuration for **4** with significantly more planar four amide donor nitrogens. However, it is by 6 kcal M^{-1} less stable than structure $\mathbf{4_A}$ in figure 5. Because of this unfavorable energy difference we believe that configuration $\mathbf{4_A}$ is more realistic.

4. Discussion

Ligand **3** was prepared in a moderate yield and, despite its highly distorted structure, its macrocyclic coordination with cobalt(III) via four deprotonated amide nitrogens was achieved. Complex **4** is believed to be a strongly distorted square-planar Co^{III} derivative. The distortion accounts for hydrolytic instability of **4** and its ease to demetalate as previously established for iron(III) TAMLs [42]. Our efforts are now concentrating on studying the coordination of other metals such as nickel and copper and evaluating the properties of the resulting compounds.

Attempts to coordinate a second metallic fragment, such as copper or ruthenium, to the peripheral bipyridine moiety were unsuccessful. However, this negative result could be anticipated considering the above-mentioned DFT-optimized structure. The lone pairs of the bipyridine nitrogens are oppositely directed making impossible the bidentate coordination of a metal center.

Addition and/or rapid exchange of aqueous ligands is relevant to catalytic reactivity. Therefore, DFT analysis of structural changes of **4** induced by axial ligation of aqueous ligands is of particular interest. It is clearly seen in figure 5 that consecutive ligation by two H_2O molecules introduces "non-linear" structural variations. Though addition of one water molecule to $\mathbf{4_A}$ to form $\mathbf{4_B}$ destabilizes the complex, two water molecules bring about the energetic stabilization of $\mathbf{4_C}$, and "in-plane" optimization of the amide nitrogens. Geometry close to ideal was predicted in terms of a near orthogonal distribution of $Co–N_{amide}$ and $Co–O_{water}$ bonds as shown for $\mathbf{4_C}$ in figure 5. The axial $Co–OH_2$ distance of ca. 1.95 Å for both water molecules is quite reasonable for the axial H_2O bond with cobalt. The existence of $\mathbf{4_C}$ with an energy minimum suggests that $\mathbf{4_C}$ might be a dominating species in aqueous solution similar to iron(III) TAMLs, which are square pyramidal as solids but exist as octahedral diaqua species in water [42].

5. Conclusion

The cobalt(III) complex with a new TAML incorporating the peripheral 2,2′-bipyridine unit is described. Though the ligand geometry is rather unfavorable for the formation of macrocyclic complex, the Co^{III} containing compound obtained after deprotonation of the N–H bonds by *n*-BuLi is stable and slightly soluble in alcohols. Similar iron(III) complex could not obtained. The macrocyclic complex of Co^{III} was explored by DFT and a strongly distorted square-planar geometry is suggested.

Acknowledgements

Financial support from DGAPA-UNAM (PAPIIT Project IN204812) and CONACyT (Project 153151 and scholarship 216383 to ROSD) is acknowledged. We thank Dr Terrence J. Collins for allowing ROSD to perform some experiments in CMU and his interest to this project.

References

[1] T.J. Collins. *Acc. Chem. Res.*, **27**, 279 (1994).
[2] T.J. Collins. *Acc. Chem. Res.*, **35**, 782 (2002).
[3] T.J. Collins, S.K. Khetan, A.D. Ryabov. In *Handbook of Green Chemistry*, P.T. Anastas, R.H. Crabtree (Eds), pp. 39–77, Wiley-VCH Verlag GmbH & KgaA, Weinheim (2009).
[4] A.D. Ryabov, T.J. Collins. *Adv. Inorg. Chem.*, **61**, 471 (2009).
[5] A.D. Ryabov. *Adv. Inorg. Chem.*, **65**, 118 (2013).
[6] A. Chanda, A.D. Ryabov, S. Mondal, L. Alexandrova, A. Ghosh, Y. Hangun-Balkir, C.P. Horwitz, T.J. Collins. *Chem. Eur. J.*, **12**, 9336 (2006).
[7] M. Emelianenko, D. Torrejon, M.A. DeNardo, A.D. Ryabov, T.J. Collins. *J. Math. Chem.*, **52**, 1460 (2014).
[8] W.C. Ellis, C.T. Tran, M.A. Denardo, A. Fischer, A.D. Ryabov, T.J. Collins. *J. Am. Chem. Soc.*, **131**, 18052 (2009).
[9] W.C. Ellis, C.T. Tran, R. Roy, M. Rusten, A. Fischer, A.D. Ryabov, B. Blumberg, T.J. Collins. *J. Am. Chem. Soc.*, **132**, 9774 (2010).
[10] C. Panda, M. Ghosh, T. Panda, R. Banerjee, S. Sen Gupta. *Chem. Commun.*, **47**, 8016 (2011).
[11] C. Barrera, I. Zhukov, E. Villagra, F. Bedioui, M.A. Páez, J. Costamagna, J.H. Zagal. *J. Electroanal. Chem.*, **589**, 212 (2006).
[12] G. Ramírez, M. Lucero, A. Riquelme, M. Villagrán, J. Costamagna, E. Trollund, M.J. Aguirre. *J. Coord. Chem.*, **57**, 249 (2004).
[13] E. Villagra, F. Bedioui, T. Nyokong, J.C. Canales, M. Sancy, M.A. Páez, J. Costamagna, J.H. Zagal. *Electrochim. Acta*, **53**, 4883 (2004).
[14] A.D. Ryabov, R. Cerón-Camacho, O. Saavedra-Diaz, M. Denardo, A. Ghosh, R. Le Lagadec, T. Collins. *Anal. Chem.*, **84**, 9096 (2012).
[15] E.L. Demeter, S.L. Hilburg, N.R. Washburn, T.J. Collins, J.R. Kitchin. *J. Am. Chem. Soc.*, **136**, 5603 (2014).
[16] J.M.S. Cabral, J.F. Kennedy. *Bioprocess Technol.*, **14**, 73 (1991).
[17] C.G. Miller, S.W. Gordon-Wylie, C.P. Horwitz, S.A. Strazisar, D.K. Peraino, G.R. Clark, S.T. Weintraub, T.J. Collins. *J. Am. Chem. Soc.*, **120**, 11540 (2004).
[18] P.V. Bernhardt, G.A. Lawrence. In *Comprehensive Coordination Chemistry II*, J.A. McCleverty, T.J. Meyer (Eds), Vol. 6, pp. 1–145, Elsevier, Oxford (2004).
[19] S. Ozaki, H. Mimura, N. Yasuhara, M. Masui, Y. Yamagata, K. Tomita, T.J. Collins. *J. Chem. Soc., Perkin Trans. 2*, 353 (1990).
[20] J. Estrada, I. Fernández, J.R. Pedro, X. Ottenwaelder, R. Ruiz, Y. Journaux. *Tetrahedron Lett.*, **38**, 2377 (1997).
[21] Q. Knijnenburg, A.D. Horton, H. Heijden, T.M. Kooistra, D.G.H. Hetterscheid, J.M.M. Smits, B. Bruin, P.H.M. Budzelaar, A.W. Gal. *J. Mol. Catal. A: Chem.*, **232**, 151 (2005).
[22] T.C. Harrop, P.K. Mascharak. *Acc. Chem. Res.*, **37**, 253 (2004).
[23] J.A. Kovacs. *Chem. Rev.*, **104**, 825 (2004).
[24] P.K. Mascharak. *Coord. Chem. Rev.*, **225**, 201 (2002).
[25] T. Yano, T. Ozawa, H. Masuda. *Chem. Lett.*, **37**, 672 (2008).
[26] A. Miyanaga, S. Fushinobu, K. Ito, T. Wakagi. *Biochem. Biophys. Res. Commun.*, **288**, 1169 (2001).
[27] A. Ghosh, P. Ramidi, S. Pulla, S.Z. Sullivan, S.L. Collom, Y. Gartia, P. Munshi, A.S. Biris, B.C. Noll, B.C. Berry. *Catal. Lett.*, **137**, 1 (2010).
[28] S. Al-Hassan, R.J. Cameron, A.W. Curran, W.J.S. Lyall, S.H. Nicholson, D.R. Robinson, A. Stuart, C.J. Suckling, I. Stirling, H.C.S. Wood. *J. Chem. Soc., Perkin Trans. I*, 1645 (1985).
[29] C.P. Horwitz, A. Ghosh. US Patent 7060818 (2006).
[30] B.Z. Shan, Q. Zhao, N. Goswami, D.M. Eichhorn, D.P. Rillema. *Coord. Chem. Rev.*, **211**, 117 (2011).
[31] G.F. Smith, F.P. Richter. *Phenanthroline and Substituted Phenanthroline Indicators*, p. 20, The G.F. Smith Chemical, Columbus, GA (1944).
[32] B.J. Hathaway, A.E. Underhill. *J. Chem. Soc.*, 3705 (1960).
[33] M.J. Frisch, G.W. Trucks, H.B. Schlegel, G.E. Scuseria, M.A. Robb, J.R. Cheeseman, G. Scalmani, V. Barone, B. Mennucci, G.A. Petersson, H. Nakatsuji, M. Caricato, X. Li, H.P. Hratchian, A.F. Izmaylov,

J. Bloino, G. Zheng, J.L. Sonnenberg, M. Hada, M. Ehara, K. Toyota, R. Fukuda, J. Hasegawa, M. Ishida, T. Nakajima, Y. Honda, O. Kitao, H. Nakai, T. Vreven, J.A. Montgomery, J.E. Peralta, F. Ogliaro, M. Bearpark, J.J. Heyd, E. Brothers, K.N. Kudin, V.N. Staroverov, R. Kobayashi, J. Normand, K. Raghavachari, A. Rendell, J.C. Burant, S.S. Iyengar, J. Tomasi, M. Cossi, N. Rega, J.M. Millam, M. Klene, J.E. Knox, J.B. Cross, V. Bakken, C. Adamo, J. Jaramillo, R. Gomperts, R.E. Stratmann, O. Yazyev, A.J. Austin, R. Cammi, C. Pomelli, J.W. Ochterski, R.L. Martin, K. Morokuma, V.G. Zakrzewski, G.A. Voth, P. Salvador, J.J. Dannenberg, S. Dapprich, A.D. Daniels, O. Farkas, J.B. Foresman, J.V. Ortiz, J. Cioslowski, D.J. Fox. *Gaussian 09, Revision B.01*, Gaussian, Inc., Wallingford, CT, USA (2009).

[34] A.D. Becke. *J. Chem. Phys.*, **98**, 3 (1993).

[35] A.D. Becke. *Phys. Rev. A*, **38**, 3098 (1988).

[36] C. Lee, W. Yang, R.G. Parr. *Phys. Rev. B*, **37**, 785 (1988).

[37] A. Chanda, X. Shan, M. Chakrabarti, W.C. Ellis, D.L. Popescu, F. Tiago de Oliveira, D. Wang, L. Que Jr, T.J. Collins, E. Münck, E.L. Bominaar. *Inorg. Chem.*, **47**, 3669 (2008).

[38] A.V. Marenich, C.J. Cramer, D.G. Truhlar. *J. Phys. Chem. B*, **113**, 6378 (2009).

[39] D.L. Popescu, A. Chanda, M. Stadler, F. de Oliveira, A.D. Ryabov, E. Münck, E.L. Bominaar, T.J. Collins. *Coord. Chem. Rev.*, **252**, 2050 (2008).

[40] T.J. Collins, R.D. Powell, C. Slebodnick, E.S. Uffelman. *J. Am. Chem. Soc.*, **113**, 8419 (1991).

[41] W.C. Ellis. Green design, synthesis, characterization, and application of a novel family of Fe(III)-TAML peroxide activating homogeneous catalysis. PhD thesis, Department of Chemistry, Carnegie Mellon University, Pittsburgh, PA (2010).

[42] A. Ghosh, A.D. Ryabov, S.M. Mayer, D.C. Horner, D.E. Prasuhn Jr, S. Sen Gupta, L. Vuocolo, C. Culver, M.P. Hendrich, C.E.F. Rickard, R.E. Norman, C.P. Horwitz, T.J. Collins. *J. Am. Chem. Soc.*, **125**, 12378 (2003).

[43] T.J. Collins, E.S. Uffelman. *Angew. Chem. Int. Ed. Engl.*, **28**, 1509 (1989).